PIM1 inhibitor synergizes the anti-tumor effect of osimertinib via STAT3 dephosphorylation in EGFR-mutant non-small cell lung cancer

Ziyi Sun[1,2], Liang Zeng[1], Miaomiao Zhang[1], Yongchang Zhang[1], Nong Yang[1]

[1]Department of Medical Oncology, Lung Cancer and Gastrointestinal Unit, Hunan Cancer Hospital/The Affiliated Cancer Hospital of Xiangya School of Medicine, Central South University, Changsha 410006, China; [2]Hunan Key Laboratory of Translational Radiation Oncology, Hunan Cancer Hospital, and The Affiliated Cancer Hospital of Xiangya School of Medicine, Central South University, Changsha 410006, China

Contributions: (I) Conception and design: N Yang, Y Zhang; (II) Administrative support: N Yang, Y Zhang; (III) Provision of study materials or patients: L Zeng; (IV) Collection and assembly of data: Z Sun; (V) Data analysis and interpretation: Z Sun, M Zhang; (VI) Manuscript writing: All authors; (VII) Final approval of manuscript: All authors.

Correspondence to: Yongchang Zhang, MD; Nong Yang, MD. Department of Medical Oncology, Lung Cancer, and Gastrointestinal Unit, Hunan Cancer Hospital/The Affiliated Cancer Hospital of Xiangya School of Medicine, Changsha 410013, China. Email: zhangyongchang@csu.edu.cn; yangnong0217@163.com.

Background: An increasing amount of evidence has demonstrated that combined or multiple targeted therapies could bring about more durable clinical outcomes, and it is known that epidermal growth factor receptor (EGFR) tyrosine kinase inhibitor (TKI) resistance is related to bypass activation. This study aims to explore a specific solution for third-generation EGFR-TKI resistance caused by bypass activation, and to examine the antitumor effects of the combination of a novel inhibitor CX-6258 HCl with osimertinib, along with its underlining mechanisms.

Methods: A bioinformatics analysis was performed to detect the relations between the provirus integration site for Moloney murine leukemia virus 1 (PIM1) expression and prognosis of lung cancer. The EGFR-mutated lung cancer cell lines were treated with the combination of CX-6258 HCl and osimertinib to analyze cell proliferation using the Cell Counting Kit-8, colony formation, and in vivo experiments. Cell migration was analyzed using wound healing and Transwell assays. The apoptosis level was detected using Annexin V–propidium iodide flow cytometry. The expression levels of EGFR and STAT3 were determined using Western blot analysis.

Results: High expression level of PIM1 was related to the poor prognosis of non-small cell lung cancer (NSCLC). The combined administration of osimertinib and CX-6258 HCl significantly inhibited cell proliferation and migration and effectively induced apoptosis in lung cancer cells. It was more efficient in suppressing EGFR activation and phosphorylation of STAT3 compared with osimertinib treatment alone. Furthermore, it showed a durable efficacy in a xenograft model.

Conclusions: This study showed that PIM1 is a poor prognostic factor for NSCLC. CX-6258 HCl is a potential molecular inhibitor to sensitize the antitumor effects of osimertinib through the inhibiting of the phosphorylation of STAT3 in NSCLC.

Keywords: PIM1; CX-6258 HCl; non-small cell lung cancer (NSCLC); osimertinib; epidermal growth factor receptor (EGFR)

Page 2 of 15

Sun et al. PIM1 inhibitor synergizes anti-tumor effect of osimertinib

Introduction

Somatic mutations in the epidermal growth factor receptor (EGFR) gene account for approximately 15% and 40% of non-small cell lung cancer (NSCLC) in Caucasians and East Asians, respectively (1,2). The progression-free survival (PFS) of patients with EGFR-mutant lung cancer using EGFR-tyrosine kinase inhibitors (TKIs) is significantly better than the PFS of patients using traditional chemotherapy (3,4). However, in 10 months, most patients experience therapy failure due to resistance to different drugs. Therefore, an improved targeted therapy that can offer better anti-cancer outcomes needs to be explored.

PIM kinases are a class of serine/threonine kinases, which consist of 3 different isoforms (PIM1, PIM2, and PIM3). PIM1 kinase enhances tumor cell proliferation by suppressing cell cycle suppressor p27 (5). Down regulating the expression of PIM1 inhibits tumor cell proliferation through inducing cell cycle arrest in the G1 phase (6). It can also inhibit apoptosis and induce drug resistance through the phosphorylation of the Bcl-2-associated death promoter (7,8). PIM1 kinase is widely expressed in hematological malignancies and is recognized as effective carcinogenic drivers (9,10). Recent studies have found that PIM1 kinase is overexpressed in solid tumors such as prostate cancer, breast cancer, pancreatic cancer, and salivary adenoid cystic carcinoma (11-14). In most lung tumor tissues, PIM1 is upregulated, and its expression is closely linked to advanced stage and poor prognosis (15).

PIM kinases are widely overexpressed in different types of tumors and involved in many oncogenic signaling pathways (15,16). A structural analysis of x-rays showed that PIM1 contains a special hinge region used as a target region to produce inhibitors of small molecules (17). Therefore, it is conceivable that PIM1 is an ideal therapeutic target in lung cancer therapy. PIM kinases play an important role in resistance to targeted therapy, chemotherapy, and radiotherapy in many tumors (16,18), and inhibiting the expression of PIM1 can increase the sensitivity of NSCLC cells to cisplatin and gefitinib (16). However, whether the combination of PIM kinase inhibitors and EGFR-TKIs can exert a better antitumor effect compared with osimertinib on EGFR-mutated NSCLCs is uncertain.

The elevated PIM1 expression may be associated to poor lung cancer prognosis. CX-6258 HCl, a pan-PIM kinase inhibitor with robust biochemical efficiency and kinase selectivity (15), and the third-generation EGFR-TKI, osimertinib, were therefore chosen to demonstrate the additive inhibitory effects on tumors. The results could provide useful guides to clinical practice.

Methods

Bioinformatics analysis

PIM1 association result was downloaded from the Linked Omics database (http://www.linkedomics.org). This result was analyzed using the Pearson correlation test. The biological process, cellular component, and molecular function that positively correlated with PIM1, were analyzed using enrichment analysis. Oncomine (https://www.oncomine.org) was used to determine the expression level of candidate genes in lung cancer, and PROGgeneV2 (http://genomics.jefferson.edu/proggene/) was used to determine the prognostic significance of PIM1.

Cell lines and reagents

Osimertinib and CX-6258 HCl were purchased from Selleck Chemicals (TX, USA). EGF was obtained from Sigma-Aldrich (St. Louis, MO, USA). Human NSCLC cell lines NCI-H1975 (amplified EGFR-T790M/del19) and PC9 (amplified EGFR-del19) were purchased from the Cell Bank of the Chinese Academy of Sciences (Shanghai, China). The cells were grown in Roswell Park Memorial Institute-1640 Medium (RPMI-1640, Gibco, USA) supplemented with 10% fetal bovine serum (FBS, Gibco, USA) 100 U/mL penicillin, and 100 μg/mL streptomycin. The cells were kept in a humidified incubator at 37 ℃ in the presence of 5% CO_2.

Cell proliferation assay

The proliferation of NSCLC cells was measured using a Cell Counting Kit-8 (CCK-8; Dojindo, Japan) following the manufacturer's protocol. Briefly, the cells were plated at a density of 3×10^3 cells per well in 96-well plates. The cells were treated with vehicle, 2.5 or 5 μM osimertinib, 2.5 or 5 μM CX-6258 HCl, or a combination of both (2.5 or 5 μM) in H1975 and PC9 cells for 24 or 48 h after attachment to the wall overnight. Then, the culture media was changed to 10% CCK-8 solution, and the cells were incubated for 3 h at 37 ℃. The cell numbers were estimated using a spectrophotometer at 450 nm.

Colony formation assay

NSCLC cells were plated at a density of 5×10^2 cells per well in 6-well plates and allowed to adhere for 12 h. After treatment with vehicle, 5 μM CX-6258 HCl, 5 μM osimertinib, or a combination of both (5 μM) for 6 h, the medium was refreshed. The cells were cultured for 14 days, washed with phosphate-buffered saline (PBS), fixed in methanol, and stained with 0.4% crystal violet. The colonies were counted by the ImageJ software (Bethesda, MD, USA).

Wound-healing assay

The cells were plated in six-well plates and allowed to cover the well overnight. The wounds were scratched in the cell monolayer using a 10-μL micropipette tip. The floating cells and debris were rinsed with PBS. To test the effects of drugs on the migration of NSCLCs, H1975, and PC9 cells were seeded in serum-free RPMI-1640 medium with the vehicle, 5 μM CX-6258 HCl, 5 μM osimertinib, or a combination of both (5 μM). Wound healing was recorded using a microscope at 0 and 48 h.

Transwell assay

The cells were plated at a density of 5×10^4 cells in a serum-free medium in the top chamber of a Transwell (Corning, NY, USA). The lower chambers were filled with 600 μL of the complete medium with the vehicle, osimertinib, CX-6258 HCl, or a combination. The medium was refreshed 6 h later. The cells were incubated for 24 h, washed with PBS twice, fixed in methanol, and stained with 0.4% crystal violet. The average number of migrating cells was determined in 6 random high-power fields.

Apoptosis assay

Apoptosis assay was performed using an Annexin V–FITC/propidium iodide (PI) apoptosis detection kit (Vazyme Biotech Co., Ltd, Nanjing, China) according to the manufacturer's protocols. Briefly, the cells were plated in six-well plates overnight and treated with vehicle, 5 μM CX-6258 HCl, 5 μM osimertinib, or a combination of both (5 μM). After 24 h of treatment, the cells were collected and washed with PBS twice. They were stained with Annexin V–FITC and PI for 15 min. The cell apoptosis was analyzed using flow cytometry (BD Biosciences, FACS Calibur).

Western blot analysis

The cells were plated in six-well plates until 80% density was achieved. Osimertinib or CX-6258 HCl was then added for 6 h, following which the cells were stimulated for 15 min with 10 ng/mL EGF (Sigma-Aldrich, St. Louis, MO, USA). The cells were lysed with RIPA buffer containing complete protease inhibitor cocktail and phosphatase inhibitor (Roche Diagnostics, IN, USA). Western blot analysis was performed on whole-cell extracts using primary antibodies against PIM1 (Abcam, Cambridge, MA, USA), EGFR, STAT3, ERK, AKT, phospho-EGFR, phospho-STAT3, phospho-ERK, phospho-AKT, PARP, caspase-3 (Cell Signaling Technology, Danvers, MA, USA), GAPDH, and α-tubulin (Proteintech, Wuhan, Hubei, China). The protein bands were visualized using the enhanced chemiluminescence (ECL) detection system (Beyotime Institute of Biotechnology, Shanghai, China) according to the manufacturer's protocols.

Xenograft model

Six-week-old female BALB/c nu/nu mice were purchased from Hunan SJA Laboratory Animal Co., Ltd. (Changsha, China). They were subcutaneously inoculated into the right flank with 5×10^6 NCI-H1975 cells (Day 1). After the tumor had grown to around 200–300 mm^3 of tumor volume (TV), the mice were randomly allocated into 4 groups: control, osimertinib, CX-6258 HCl, and osimertinib combined with CX-6258 HCl. Osimertinib (1 mg/kg in 1% DMSO) and CX-6258 HCl (25 mg/kg in 1% DMSO) were given daily by oral gavage. The tumors were measured using a Vernier caliper 3 times a week. The antitumor activity was evaluated using TV, which was estimated from the following equation: $TV = AB^2/2$ (where A and B are tumor length and width, respectively). The mice were euthanized by cervical dislocation at the end of the experiments. All experiments involving animals were performed following ARRIVE guidelines and after the approval of the local ethical committee of Hunan Cancer Hospital.

Immunohistochemistry

The tumor slides were fixed in 10% buffered formalin solution and embedded in paraffin. The antigens were probed with caspase-3 (Proteintech), p-EGFR (Cell Signaling Technology), or PIM1 (Abcam) and detected with peroxidase-conjugated secondary antibody (Dako, K5007).

Page 4 of 15

Sun et al. PIM1 inhibitor synergizes anti-tumor effect of osimertinib

The degree of immunostaining was evaluated using the proportion of positively stained tumor cells and staining intensities. This project has been reviewed and approved by Hunan Cancer Hospital IRB Committee (Approval number: 201902651).

Statistical analysis

Data were expressed as mean ± standard deviation (SD). Statistical analysis was conducted using SPSS 16.0 software. P values were calculated using the unpaired two-tailed Student t-test or one-way ANOVA test. The differences were considered significant at P values less than 0.05.

Results

High expression of PIM1 was related to the poor prognosis of lung cancer

Increasing evidence has shown that PIM1 kinase is an effective carcinogenic driver of different malignant tumors (17,19). The Oncomine database showed that the expression level of the PIM1 gene was higher in different pathological types of lung cancer compared with normal tissues (*Figure 1A*). The PIM1 association result was analyzed using the Pearson correlation test on the Linked Omics database (*Figure 1B*). Meanwhile, the survival analysis of PIM1 from the GSE30219 and GSE 3141 datasets was performed in the PROGgeneV2 database, revealing that high the expression of the PIM1 gene had a significantly negative correlation with overall survival (*Figure 1C,D*). Furthermore, we found that cell proliferation and cell cycle were positively correlated with PIM1. This suggests that PIM1 might promote cell proliferation via modulating cell cycle (*Figures S1,S2*). These findings indicate that PIM1 is a potential oncogenic biomarker in lung cancer and targeting PIM1 might be an ideal approach in the targeted therapy of lung cancer.

CX-6258 HCl combined with osimertinib inhibited the proliferation of H1975 and PC9 cells

The effects of the combination of osimertinib with CX-6258 HCl on the proliferation of H1975 (EGFR-T790M) and PC9 (exon 19 deletions) lung cancer cells were investigated. As shown in *Figure 2A,B*, both H1975 and PC9 cells were more sensitive to osimertinib than to CX-6258 HCl. The administration of osimertinib combined with CX-6258

HCl was more effective in suppressing cell viability in a dose- and time-dependent manner (*Figure 2A,B,C,D*). The colony formation assay showed that the combined treatment exerted an additive inhibitory effect on colony formation compared with osimertinib alone (*Figure 2E,F*). The colonies in the combined-treatment group were much smaller and fewer compared with the colonies in the control group (*Figure 2G,H*). These findings showed that CX-6258 HCl, combined with osimertinib, had a better growth-inhibitory effect compared with either inhibitor used alone.

CX-6258 HCl combined with osimertinib inhibited cell migration in H1975 and PC9 cells

The wound-healing assay was used to detect the effects of combined administration on cell migration. Treatment with the combination of osimertinib and CX-6258 HCl for 48 h significantly increased the open space compared with single administration (*Figure 3A,B*). Results presented in *Figure 3C,D* showed that the combination inhibited cell migration in H1975 and PC9 cells more effectively in quantification. In the transwell assay, the combination elicited a strong inhibitory effect on tumor cell migration (*Figure 3E,F*). Quantification is shown in *Figure 3G,H*. Taken together, the results indicate that the combination of osimertinib and CX-6258 HCl can exert additively inhibitory effects on cell migration.

CX-6258 HCl combined with osimertinib induced apoptosis

An Annexin V–FITC/PI apoptosis detection kit was used to analyze the effect of the combination of osimertinib and CX-6258 HCl on apoptosis. Most cells in the control group remained intact. However, apoptosis was induced in the osimertinib-treated H1975 cells from 5.1%±0.1% to 11.2%±0.9% (P<0.001, *Figure 4A,B*), and in the osimertinib-treated PC9 cells from 6.9%±0.4% to 11.5%±1.2% (P<0.001, *Figure 4C,D*). The apoptotic rate increased to 16.0%±0.3% and 16.2%±0.5%, respectively, in the CX-6258 HCl-treated H1975 and PC9 cells compared with the osimertinib-treated cells. The combined treatment produced the most significant effect on apoptosis, with the apoptotic rate 20.6%±0.7% in H1975 cells and 24.4%±0.5% in PC9 cells (P<0.001, *Figure 4B,D*). These data showed that CX-6258 HCl alone not only induced the apoptosis of EGFR-mutated NSCLC cell lines but also significantly increased the apoptotic rate when combined
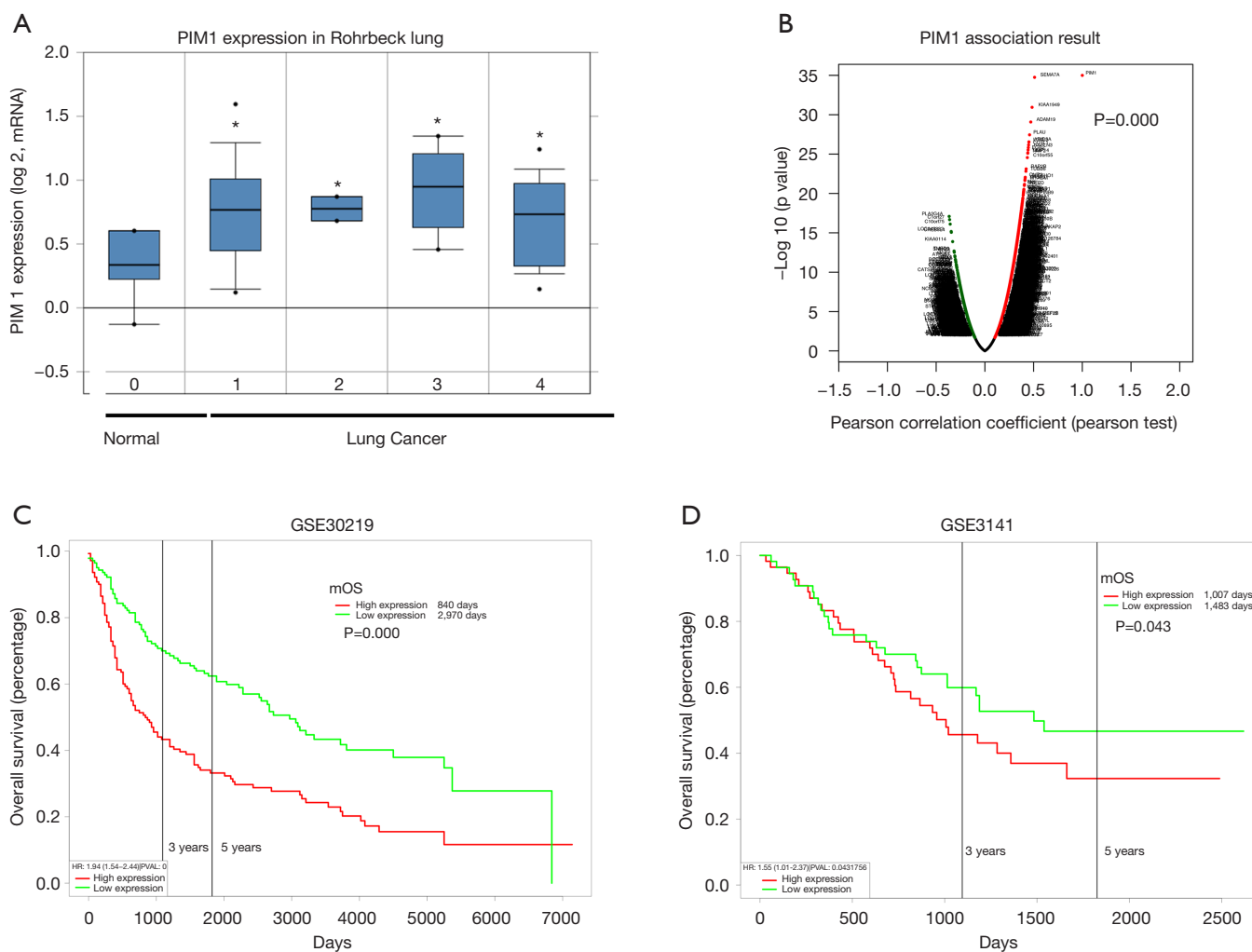
Figure 1 High expression of PIM1 was related to the poor prognosis of lung cancer. (A) PIM1 expression was upregulated in different pathological types of lung cancer. (B) The PIM1 association result was downloaded from the Linked Omics database. (C) Patients with high expression of PIM1 had significantly worse survival compared with low-expression patients (n=282, P<0.0001, HR =1.94). (D) Patients with the high expression of PIM1 had significantly worse survival compared with low-expression patients (n=111, P<0.05, HR =1.55). *, P<0.05. PIM1, provirus integration site for Moloney murine leukemia virus 1.

with osimertinib. Furthermore, the expression levels of cleaved PARP and cleaved caspase-3 were significantly higher in the combined-treatment group compared with the untreated and single-treatment groups (*Figure 5*). These findings confirm that CX-6258 HCl has great potential in combination with other drugs to promote apoptosis.

CX-6258 HCl combined with osimertinib blocked the phosphorylation of EGFR and STAT3

To elucidate the role of CX-6258 HCl and osimertinib in

H1975 and PC9 cells, the expression levels of key proteins related to STAT and EGFR pathways were assessed. CX-6258 HCl decreased the expression level of PIM1 and phosphorylation levels of STAT3. The combination resulted in a more visible suppression compared with single administration (*Figure 5*). The expression of EGFR and its downstream molecules AKT and ERK was detected. Osimertinib effectively inhibited the phosphorylation of p-EGFR, p-ERK, and p-AKT, but did not alter the total protein levels of EGFR, ERK, and AKT in H1975 and PC9 cell lines. However, the combination of CX-6258
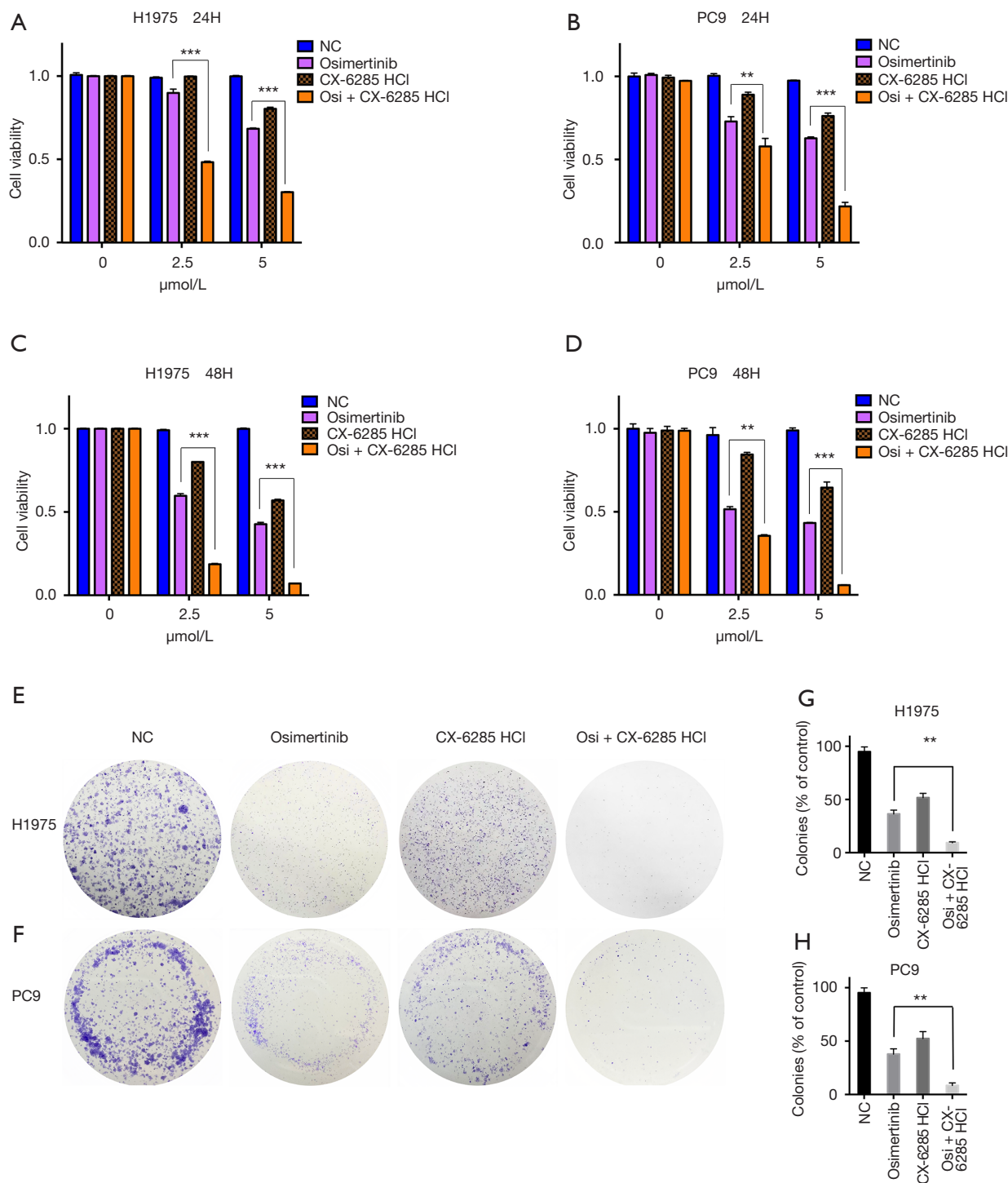
Page 6 of 15

Sun et al. PIM1 inhibitor synergizes anti-tumor effect of osimertinib

Figure 2 A combination of CX-6258 HCl and osimertinib inhibited cell proliferation. (A,C) Cell proliferation was measured using CCK-8 assay with the vehicle, 2.5 or 5 μM osimertinib, 2.5 or 5 μM CX-6258 HCl, or a combination of both (2.5 or 5 μM) in H1975 cells for 24 or 48 h. (B,D) Cell proliferation was measured using CCK-8 assay with the vehicle, 2.5 or 5 μM osimertinib, 2.5 or 5 μM CX-6258 HCl, or a combination of both (2.5 or 5 μM) in PC9 cells for 24 or 48 h. (E,F) Colony formation assay for H1975 and PC9 cell lines treated with vehicle, 5 μM CX-6258 HCl, 5 μM osimertinib, or a combination of both (5 μM). (G) Colony formation assay for H1975 cells shown as the mean ± SD (n=3). (H) Colony formation assay for PC9 cells shown as the mean ± SD (n=3). **, P<0.01, ***, P<0.001. SD, standard deviation.
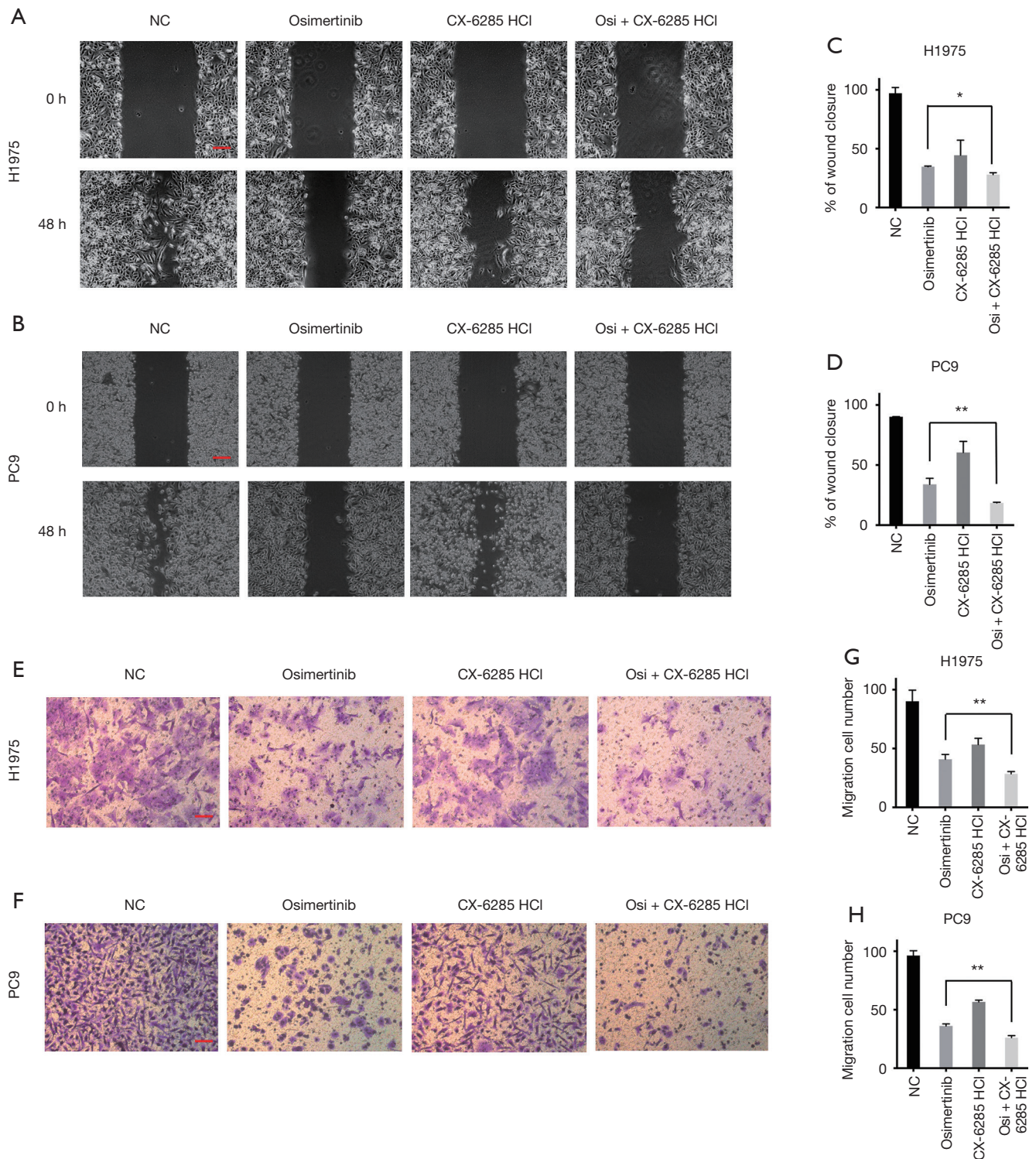
Figure 3 CX-6258 HCl, combined with osimertinib, inhibited cell migration. (A,B) Representative results of a wound-healing assay in cells treated with vehicle, 5 μM CX-6258 HCl, 5 μM osimertinib, or a combination of both (5 μM) for 48 h. Bar =100 μm. (C,D) Columns represent means ± SD from 3 independent experiments. (E,F) Representative results of Transwell assay in cells treated with vehicle, 5 μM CX-6258 HCl, 5 μM osimertinib, or a combination of (5 μM) for 6 h. Bar =20 μm. (G,H) Columns represent means ± SD from 3 independent experiments. *, P<0.05, **, P<0.01.

Page 8 of 15

Sun et al. PIM1 inhibitor synergizes anti-tumor effect of osimertinib
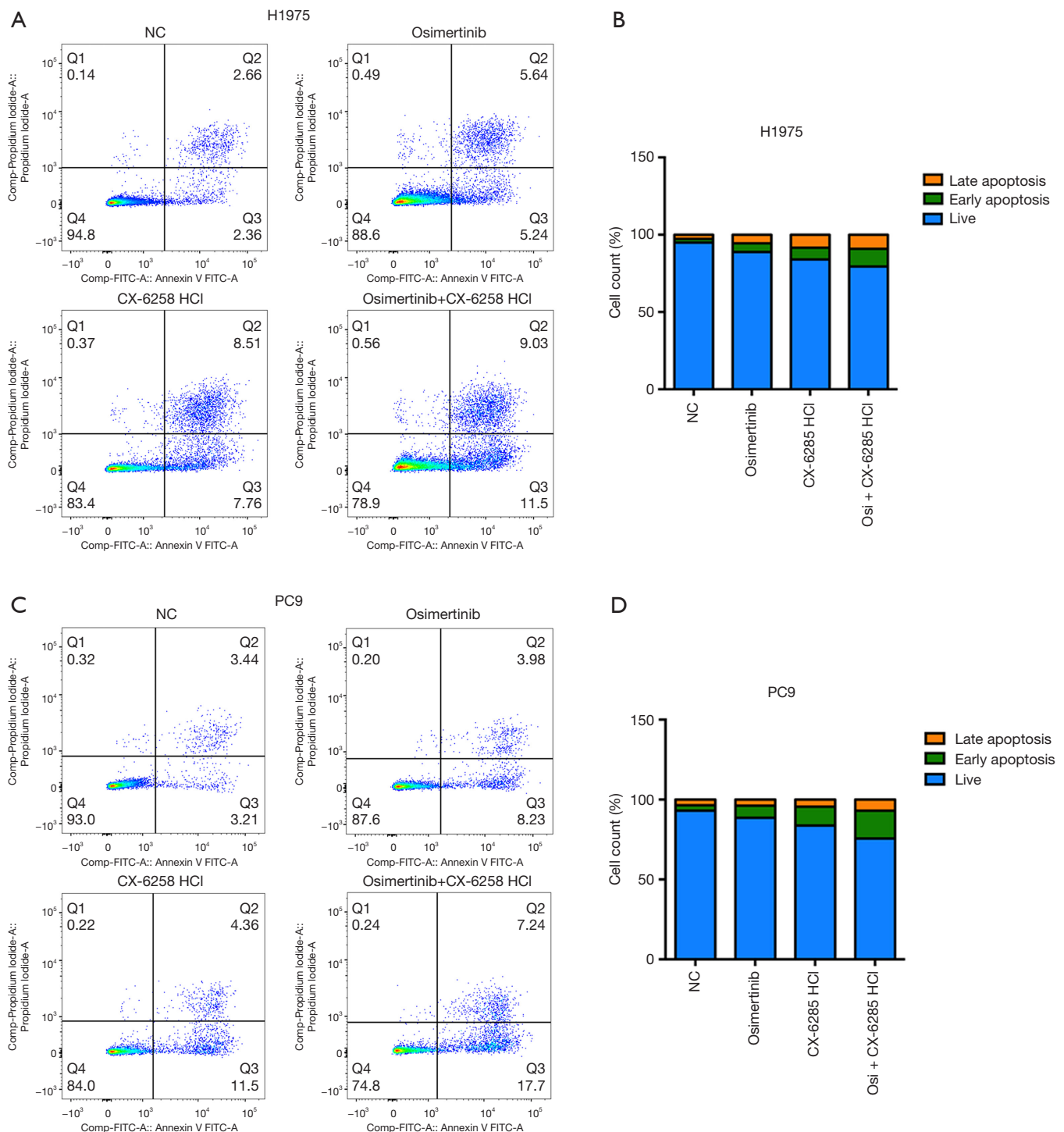
Figure 4 CX-6258 HCl combined with osimertinib induced apoptosis. (A,C) H1975 and PC9 cells were treated for 24 h with the following agents: vehicle, 5 μM CX-6258 HCl, 5 μM osimertinib, or a combination of both (5 μM). Apoptosis assay was performed using an Annexin V–FITC/PI apoptosis detection kit. (B,D) Quantification of the fractions of early- and late-resistant apoptotic cells is shown in the histograms. The experiment was repeated 3 times. The Student's *t*-test was used between the osimertinib group and the combination group.
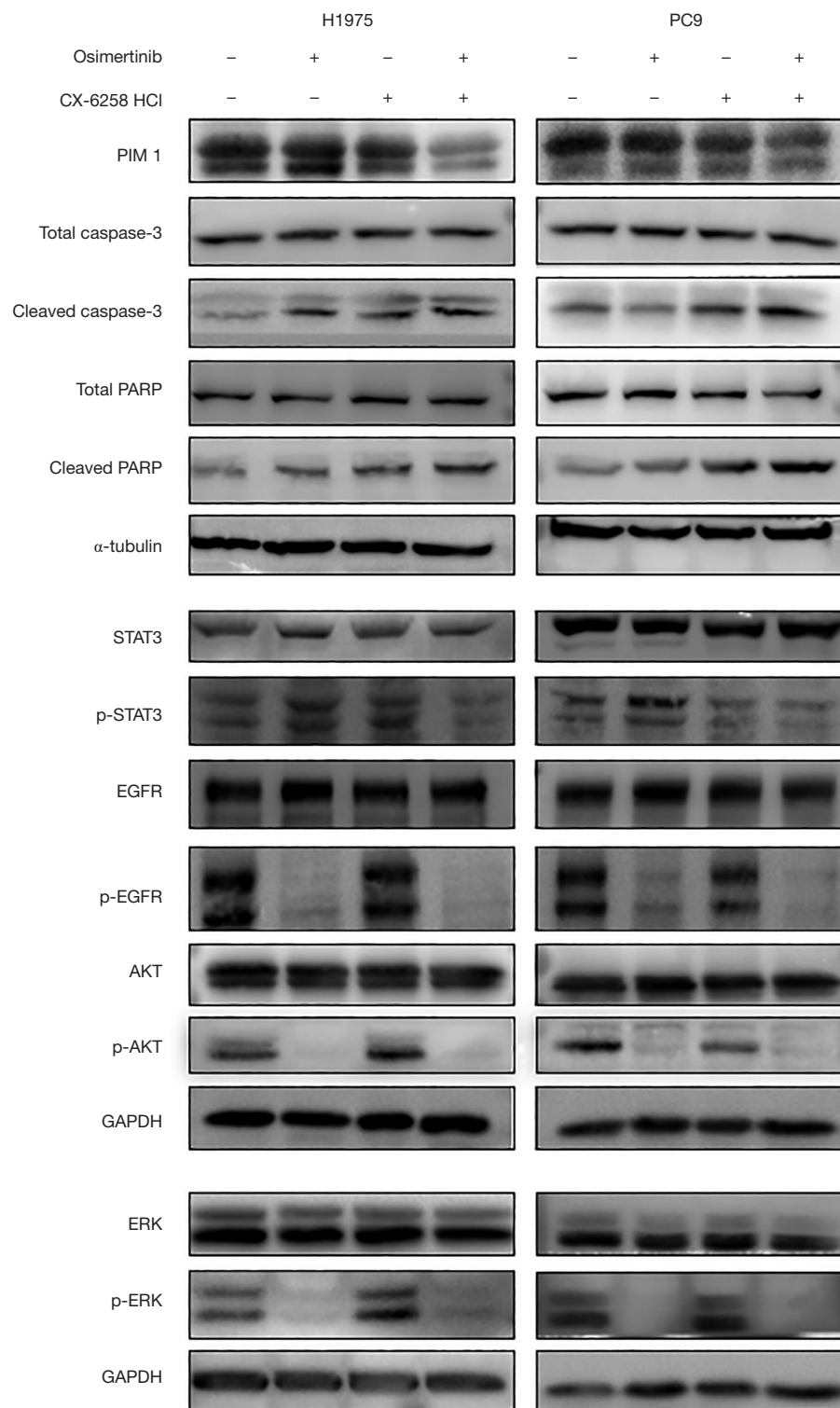
Figure 5 Effect of osimertinib on the expression of PIM1, caspase 3, and PARP, and the total levels or phosphorylation inhibition of STAT3, EGFR, AKT, and ERK. H1975 and PC9 cells were treated with vehicle, 5 µM CX-6258 HCl, 5 µM osimertinib, or a combination of both (5 µM) for 6 h following EGF stimulation, and the extracts were blotted using the indicated antibodies. EGFR, epidermal growth factor receptor.

HCl and osimertinib blocked the phosphorylation of EGFR, ERK, and AKT and caused the weaker expression of p-EGFR compared with osimertinib alone (*Figure 5*). These results showed that the combination suppressed the phosphorylation of EGFR.

CX-6258 HCl combined with osimertinib inhibited tumor growth in a xenograft model

The NCI-H1975 xenograft model was used to evaluate whether the combination had an antitumor effect *in vivo*. H1975 cells were implanted in the flanks of BALB/c nu/nu mice, and the animals were randomized into 4 groups until tumors grew to around 200–300 mm^3 of TV. The results showed that the combined administration did not gain satisfactory achievements in the first week. However, it did eventually suppress the growth of the H1975 subcutaneous tumor (*Figure 6A,B*). Meanwhile, the safety of the combined administration was evaluated by taking the weight of mice. The combined administration did not significantly influence body weight (P>0.05, *Figure 6C*). Isolated tumors from each treatment group were presented in *Figure 6D*.

Next, mice were euthanized, and the tumors were excised. The expression of PIM1, p-EGFR, and caspase-3 was detected in tumor tissues using immunohistochemistry. The number of caspase 3+ tumor cells increased with each single drug administration. As expected, it was further increased in the combined administration group (*Figure 7*). The results revealed a strong expression of p-EGFR in tumor cells of the control group. CX-6258 HCl slightly decreased the expression level of p-EGFR. However, both osimertinib and combined administration further decreased the expression of p-EGFR (*Figure 7*). The expression level of PIM1 significantly decreased in tumor cells treated with CX-6258 HCl (*Figure 7*). These data were consistent with the *in vitro* data.

Conclusions

Like other targeted therapies, resistance to EGFR-TKI is inevitable. Many studies have discovered the molecular mechanism underlying acquired drug resistance to EGFR inhibitors. However, little is known about the ways to delay or overcome this resistance. Increasing evidence has demonstrated that combined or multiple targeted therapies can help overcome EGFR-TKI resistance. This novel study showed that the combination of CX-6258 HCl and osimertinib exerted a synergetic anti-tumor effect *in vivo*

and *in vitro*; the JAK/STAT3 pathway was also suppressed (*Figure 8*).

PIM kinases are responsible for the improvement in sensitivity to tumor inducers (9). The expression level of PIM1 in different pathologic types of lung cancer was higher than that in normal lung tissue. Moreover, the high expression of PIM1 might correlate with the poor prognosis of NSCLC. These findings may offer clinical support for subsequent research. CX-6258 HCl is a pan-PIM kinase inhibitor that selectively inhibits all 3 PIM kinases (PIM1, PIM2, and PIM3) (15); it has the most substantial inhibitory effect on PIM1.

Sustaining proliferative signaling and promoting invasion and metastasis are 2 significant features of tumors (20). In the present study, the proliferation and migration of EGFR-mutated cells were significantly repressed with the combined administration of 2 inhibitors compared with the control or single administration. Such results were linked to the combination of osimertinib and CX-6258 HCl for inhibition of EGFR activation. EGFR is well known as a receptor for the epithelial growth factor in cell proliferation, invasion, and metastasis as well as signal transduction. This study demonstrated that the combination of osimertinib and CX-6258 HCl significantly inhibited the expression of p-EGFR compared with osimertinib alone. Additionally, the expression of p-EGFR was detected in the tumor tissue from xenograft models using immunohistochemistry, which was consistent with the results in vitro. These results are related to the fact that PIM kinases promoted tumor cell proliferation by regulating cell cycle suppressors p27 and p21 (21,22) and regulated migration through inhibiting the JAK/STAT pathway (23,24). Also, the combined treatment markedly reduced the tumor size in an H1975 xenograft model. Meanwhile, minimal bodyweight loss or toxicity was seen in the combined treatment group, suggesting that the simultaneous inhibition of PIM kinases led to more durable antitumor effects.

Programmed cell death by apoptosis is an important mechanism of homeostatic balance. Impaired apoptosis plays a central role in cancer development (25-27). PIM kinases are known to prevent apoptosis through the direct phosphorylation of BAD and the release of anti-apoptotic Bcl-2 protein (28,29). In this study, Annexin V–FITC/PI double staining results revealed that the combination effectively induced apoptosis in H1975 and PC9 cells. As the main effector caspase, caspase-3 is a common downstream effector of multiple apoptotic pathways and occupies a core position in the process of apoptosis.
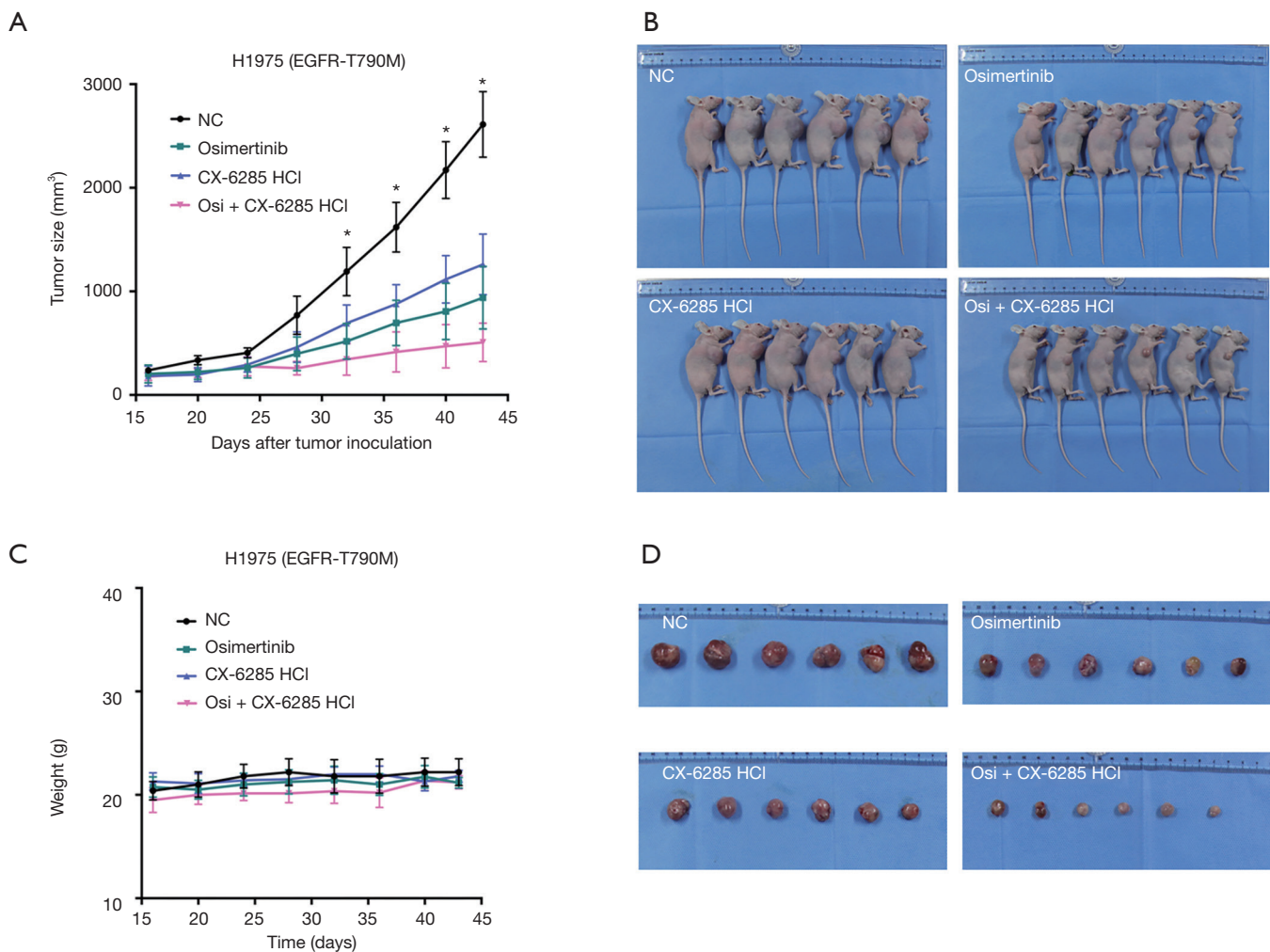
Figure 6 CX-6258 HCl combined with osimertinib inhibited tumor growth in a xenograft model. BALB/c nu/nu mice were subcutaneously inoculated into the right flank with 5×10^6 cells NCI-H1975 cells (Day 1). The mice were randomly distributed into 4 groups: control, osimertinib, CX-6258 HCl, and osimertinib combined with CX-6258 HCl. Osimertinib (1 mg/kg in 1% DMSO) and CX-6258 HCl (25 mg/kg in 1% DMSO) were given daily by oral gavage. (A) Volume changes in the subcutaneously implanted tumors in each group since the day of the start of administration. Data are represented as means ± SD, (n=6, *, P<0.05). (B) Anti-tumor effects of CX-6258 HCl combined with osimertinib on H1975-bearing mice. (C) Change in body weight of subcutaneous tumor-bearing mice in each group. The weights were measured using a Vernier caliper 3 times a week. No difference was observed among the different groups (P>0.05). (D) Tumors isolated from each treatment group 26 days after different treatments.

Once activated, caspase-3 has a high proteolytic ability to degrade intracellular target substances on a large scale and eventually cause irreversible cell death (30). The activation of caspase-3 depends heavily on the release of cyt-c (31,32). However, PIM kinases increase the release of Bcl-2 (33,34). The overexpressed Bcl-2 forms a heterodimer with BAX, which closes the mitochondrial permeability transition pore and inhibits the delivery of cyt-c, thereby hindering the activation of caspase-3 (35,36). The combination of osimertinib and CX-6258 HCl caused the increased expression of cleaved caspase-3 and cleaved PARP, further proving that CX-6258HCl exerted a robust synergistic action by promoting apoptosis. In line with the *in vitro* experiment, the expression of activated caspase-3 was upregulated.

The third-generation EGFR-TKIs bind covalently to a cysteine on codon 797, which not only works on the original mutation but also targets the most common mode
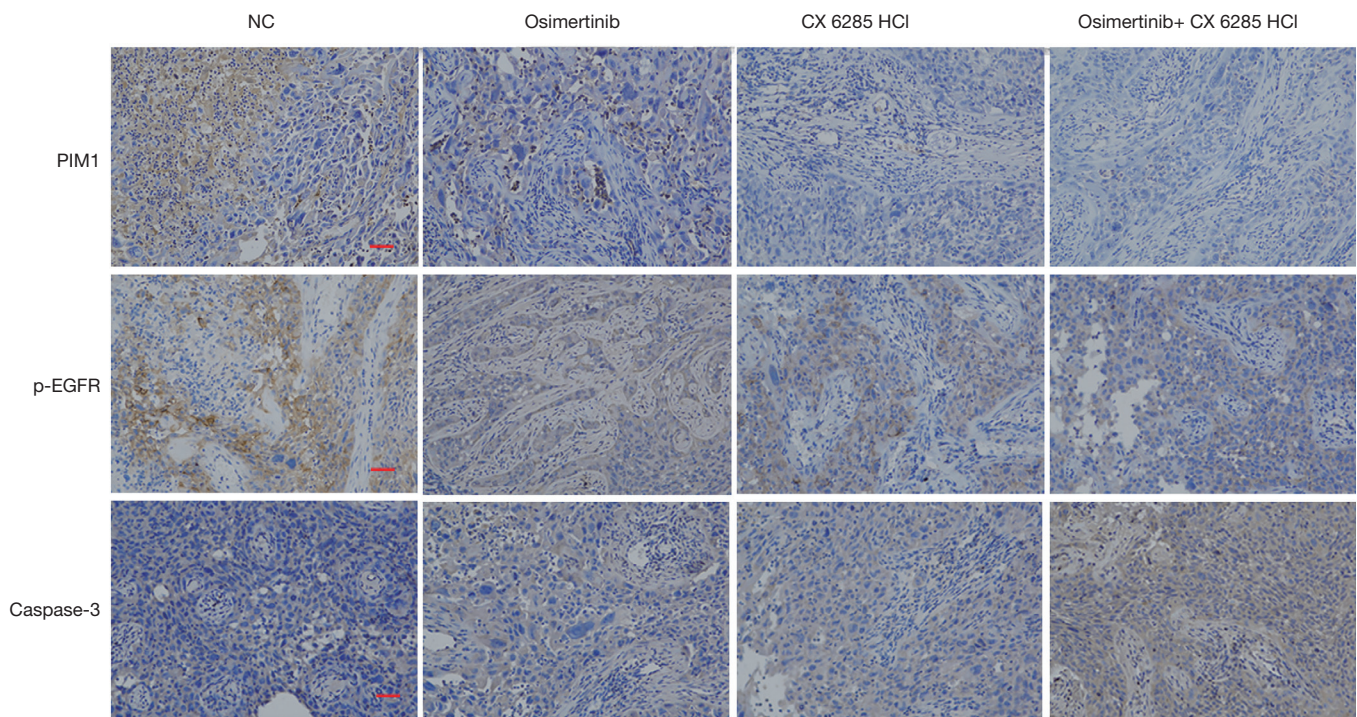
Page 12 of 15

Sun et al. PIM1 inhibitor synergizes anti-tumor effect of osimertinib

Figure 7 CX-6258 HCl combined with osimertinib inhibited the expression of PIM1, p-EGFR, and caspase-3 in the tumor tissue. Immunohistochemistry images for PIM1, p-EGFR, and caspase-3 staining of tumor tissue in BALB/c nu/nu mice. All images were 20× magnification; bar =50 µm.

of resistance T790M-EGFR (37,38). In this study, two NSCLC cell lines with different mutations were selected to observe the efficacy of the combination of osimertinib and CX-6258 HCl. Acquired resistance of EGFR-TKIs leads to the failure of clinical treatment in EGFR-mutated NSCLC. Hata *et al.* found that the inhibitory effect of the third-generation irreversible EGFR inhibitor was stronger on early-resistant PC9-GR2 cells than on late-resistant PC9-GR3 cells, which was attributed to the downregulation of Bcl-2 interacting mediator of cell death (BIM) in late-resistant PC9-GR3 cells (39). A significant feature of drug-resistant cells is the evasion of drug-induced apoptosis, especially in late-resistant cells. Thus, anti-apoptotic inhibitors can restore the sensitivity of resistant clones to drugs. Also, MacKeigan found that STAT3 was overexpressed in EGFR-mutant NSCLC cells, but EGFR-TKI did not inhibit the activation of STAT3. The inhibitors of JAK2 not only blocked the activation of STAT3 but also significantly enhanced the effect of erlotinib to repress the formation of clones and the growth of xenografts *in vivo* (40,41). As a highly selective pan-PIM inhibitor, CX-

6258 HCl possesses the capability of inducing apoptosis, besides directly binding to STAT3 and reducing its phosphorylation (42). Therefore, the expression of STAT3 and p-STAT3 was evaluated in the present study. The combination of CX-6258 HCl and osimertinib significantly downregulated the expression of p-STAT3, suggesting that the pan-PIM kinase inhibitor with EGFR-TKI suppressed tumor growth via targeting the STAT3 pathway in NSCLC. Nevertheless, it was not possible to verify the hypothesis that the joint method could reverse osimertinib resistance because the development of the osimertinib-resistant cell lines and animal models was not very successful.

In conclusion, this study was novel in reporting the antitumor effect of the combination of pan-PIM inhibitor and osimertinib on EGFR-mutated NSCLC cell lines. The interventions designed in this study not only more efficiently inhibited the phosphorylation of EGFR but also restored drug-induced apoptosis and repressed other alternative pathways. Therefore, CX-6258 HCl can act synergistically with other targeted drugs to exert more powerful anti-tumor effects.
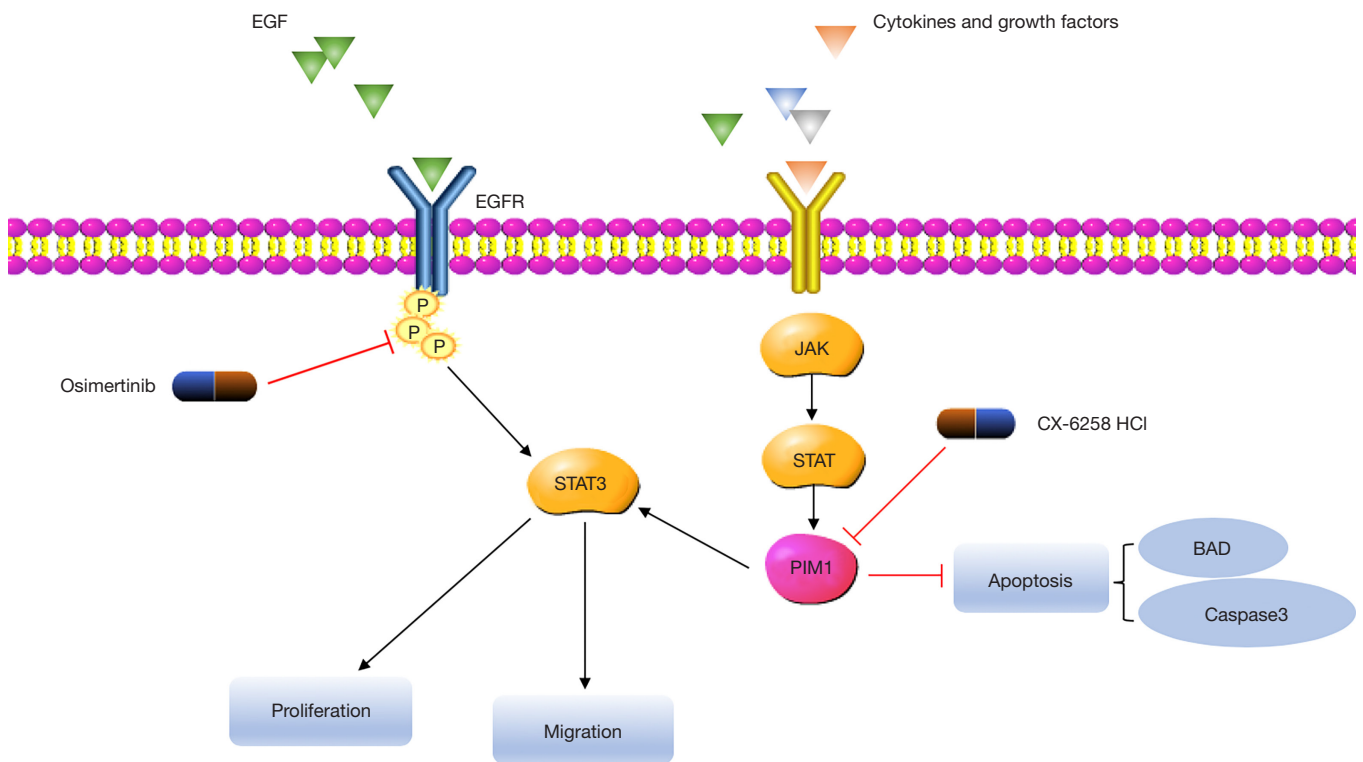
Figure 8 Pattern diagram.

Footnote

Conflicts of Interest: YZ serves as an unpaid editorial board member of *Annals of Translational Medicine* from May 2019 to Apr 2021. The other authors have no conflicts of interest to declare.

Ethical Statement: The authors are accountable for all aspects of the work in ensuring that questions related to the accuracy or integrity of any part of the work are appropriately investigated and resolved. Institutional review board approval was obtained from Hunan Cancer Hospital IRB Committee (Approval number: 201902651).

Open Access Statement: This is an Open Access article distributed in accordance with the Creative Commons Attribution-NonCommercial-NoDerivs 4.0 International License (CC BY-NC-ND 4.0), which permits the non-commercial replication and distribution of the article with the strict proviso that no changes or edits are made and the original work is properly cited (including links to both the formal publication through the relevant DOI and the license). See: https://creativecommons.org/licenses/by-nc-nd/4.0/.

References

1. Kris MG, Johnson BE, Berry LD, et al. Using multiplexed assays of oncogenic drivers in lung cancers to select targeted drugs. JAMA 2014;311:1998-2006.

2. Yatabe Y, Kerr KM, Utomo A, et al. EGFR mutation testing practices within the Asia Pacific region: results of a multicenter diagnostic survey. J Thorac Oncol 2015;10:438-45.

3. Goss G, Tsai CM, Shepherd FA, et al. Osimertinib for pretreated EGFR Thr790Met-positive advanced non-small-cell lung cancer (AURA2): a multicentre, open-label,

Page 14 of 15

Sun et al. PIM1 inhibitor synergizes anti-tumor effect of osimertinib

single-arm, phase 2 study. Lancet Oncol 2016;17:1643-52.

4. Cho JH, Lim SH, An HJ, et al. Osimertinib for Patients With Non-Small-Cell Lung Cancer Harboring Uncommon EGFR Mutations: A Multicenter, Open-Label, Phase II Trial (KCSG-LU15-09). J Clin Oncol 2020;38:488-95.

5. Zhang X, Song M, Kundu JK, et al. PIM Kinase as an Executional Target in Cancer. J Cancer Prev 2018;23:109-16.

6. Wang Y, Zhou X, Shan B, et al. Downregulation of microRNA33a promotes cyclindependent kinase 6, cyclin D1 and PIM1 expression and gastric cancer cell proliferation. Mol Med Rep 2015;12:6491-500.

7. Zhang X, Sun Y, Wang P, et al. Reduced pim-1 expression increases chemotherapeutic drug sensitivity in human androgen-independent prostate cancer cells by inducing apoptosis. Exp Ther Med 2019;18:2731-8.

8. Zhu Q, Li Y, Guo Y, et al. Long non-coding RNA SNHG16 promotes proliferation and inhibits apoptosis of diffuse large B-cell lymphoma cells by targeting miR-497-5p/PIM1 axis. J Cell Mol Med 2019;23:7395-405.

9. van Lohuizen M, Verbeek S, Krimpenfort P, et al. Predisposition to lymphomagenesis in pim-1 transgenic mice: cooperation with c-myc and N-myc in murine leukemia virus-induced tumors. Cell 1989;56:673-82.

10. Mondello P, Cuzzocrea S, Mian M. Pim kinases in hematological malignancies: where are we now and where are we going? J Hematol Oncol 2014;7:95.

11. Zhu X, Xu JJ, Hu SS, et al. Pim-1 acts as an oncogene in human salivary gland adenoid cystic carcinoma. J Exp Clin Cancer Res 2014;33:114.

12. Santio NM, Eerola SK, Paatero I, et al. Pim Kinases Promote Migration and Metastatic Growth of Prostate Cancer Xenografts. PLoS One 2015;10:e0130340.

13. Brasó-Maristany F, Filosto S, Catchpole S, et al. PIM1 kinase regulates cell death, tumor growth and chemotherapy response in triple-negative breast cancer. Nat Med 2016;22:1303-13.

14. Xu J, Xiong G, Cao Z, et al. PIM-1 contributes to the malignancy of pancreatic cancer and displays diagnostic and prognostic value. J Exp Clin Cancer Res 2016;35:133.

15. Cen B, Xiong Y, Song JH, et al. The Pim-1 protein kinase is an important regulator of MET receptor tyrosine kinase levels and signaling. Mol Cell Biol 2014;34:2517-32.

16. Song JH, Singh N, Luevano LA, et al. Mechanisms Behind Resistance to PI3K Inhibitor Treatment Induced by the PIM Kinase. Mol Cancer Ther 2018;17:2710-21.

17. Ye C, Zhang C, Huang H, et al. The Natural Compound Myricetin Effectively Represses the Malignant Progression of Prostate Cancer by Inhibiting PIM1 and Disrupting the PIM1/CXCR4 Interaction. Cell Physiol Biochem 2018;48:1230-44.

18. Green AS, Maciel TT, Hospital MA, et al. Pim kinases modulate resistance to FLT3 tyrosine kinase inhibitors in FLT3-ITD acute myeloid leukemia. Sci Adv 2015;1:e1500221.

19. Gao X, Liu X, Lu Y, et al. PIM1 is responsible for IL-6-induced breast cancer cell EMT and stemness via c-myc activation. Breast Cancer 2019;26:663-71.

20. Hanahan D, Weinberg RA. Hallmarks of cancer: the next generation. Cell 2011;144:646-74.

21. Weirauch U, Beckmann N, Thomas M, et al. Functional role and therapeutic potential of the pim-1 kinase in colon carcinoma. Neoplasia 2013;15:783-94.

22. Liu Z, Liu H, Yuan X, et al. Downregulation of Pim-2 induces cell cycle arrest in the G0/G1 phase via the p53-non-dependent p21 signaling pathway. Oncol Lett 2018;15:4079-86.

23. Narlik-Grassow M, Blanco-Aparicio C, Carnero A. The PIM family of serine/threonine kinases in cancer. Med Res Rev 2014;34:136-59.

24. Eerola SK, Santio NM, Rinne S, et al. Phosphorylation of NFATC1 at PIM1 target sites is essential for its ability to promote prostate cancer cell migration and invasion. Cell Commun Signal 2019;17:148.

25. Ichim G, Tait SW. A fate worse than death: apoptosis as an oncogenic process. Nat Rev Cancer 2016;16:539-48.

26. Adams JM, Cory S. The BCL-2 arbiters of apoptosis and their growing role as cancer targets. Cell Death Differ 2018;25:27-36.

27. Chin HS, Li MX, Tan IKL, et al. VDAC2 enables BAX to mediate apoptosis and limit tumor development. Nat Commun 2018;9:4976.

28. Fan YB, Li K, Huang M, et al. Design and synthesis of substituted pyrido[3,2-d]-1,2,3-triazines as potential Pim-1 inhibitors. Bioorg Med Chem Lett. 2016;26:1224-8.

29. Aziz AUR, Farid S, Qin K, et al. PIM Kinases and Their Relevance to the PI3K/AKT/mTOR Pathway in the Regulation of Ovarian Cancer. Biomolecules 2018. doi: 10.3390/biom8010007.

30. Hui KK, Kanungo AK, Elia AJ, et al. Caspase-3 deficiency reveals a physiologic role for Smac/DIABLO in regulating programmed cell death. Cell Death Differ 2011;18:1780-90.

31. Zhu X, Zhang K, Wang Q, et al. Cisplatin-mediated c-myc overexpression and cytochrome c (cyt c) release result in the up-regulation of the death receptors DR4 and

DR5 and the activation of caspase 3 and caspase 9, likely responsible for the TRAIL-sensitizing effect of cisplatin. Med Oncol 2015;32:133.

32. Jiang W, Chen Y, Li B, et al. DBA-induced caspase-3-dependent apoptosis occurs through mitochondrial translocation of cyt-c in the rat hippocampus. Mol Biosyst 2017;13:1863-73.

33. Macdonald A, Campbell DG, Toth R, et al. Pim kinases phosphorylate multiple sites on Bad and promote 14-3-3 binding and dissociation from Bcl-XL. BMC Cell Biol 2006;7:1.

34. Chen J, Kobayashi M, Darmanin S, et al. Pim-1 plays a pivotal role in hypoxia-induced chemoresistance. Oncogene 2009;28:2581-92.

35. Verma YK, Raghav PK, Raj HG, et al. Enhanced heterodimerization of Bax by Bcl-2 mutants improves irradiated cell survival. Apoptosis 2013;18:212-25.

36. Warren CFA, Wong-Brown MW, Bowden NA. BCL-2 family isoforms in apoptosis and cancer. Cell Death Dis 2019;10:177.

37. Stinchcombe TE. AZD9291 in epidermal growth factor receptor inhibitor-resistant non-small-cell lung cancer. Transl Lung Cancer Res 2016;5:92-4.

38. Herbst RS, Morgensztern D, Boshoff C. The biology and management of non-small cell lung cancer. Nature 2018;553:446-54.

39. Hata AN, Niederst MJ, Archibald HL, et al. Tumor cells can follow distinct evolutionary paths to become resistant to epidermal growth factor receptor inhibition. Nat Med 2016;22:262-9.

40. Zhang FQ, Yang WT, Duan SZ, et al. JAK2 inhibitor TG101348 overcomes erlotinib-resistance in non-small cell lung carcinoma cells with mutated EGF receptor. Oncotarget 2015;6:14329-43.

41. Gao SP, Chang Q, Mao N, et al. JAK2 inhibition sensitizes resistant EGFR-mutant lung adenocarcinoma to tyrosine kinase inhibitors. Sci Signal 2016;9:ra33.

42. Kuang X, Xiong J, Wang W, et al. PIM inhibitor SMI-4a induces cell apoptosis in B-cell acute lymphocytic leukemia cells via the HO-1-mediated JAK2/STAT3 pathway. Life Sci 2019;219:248-56.
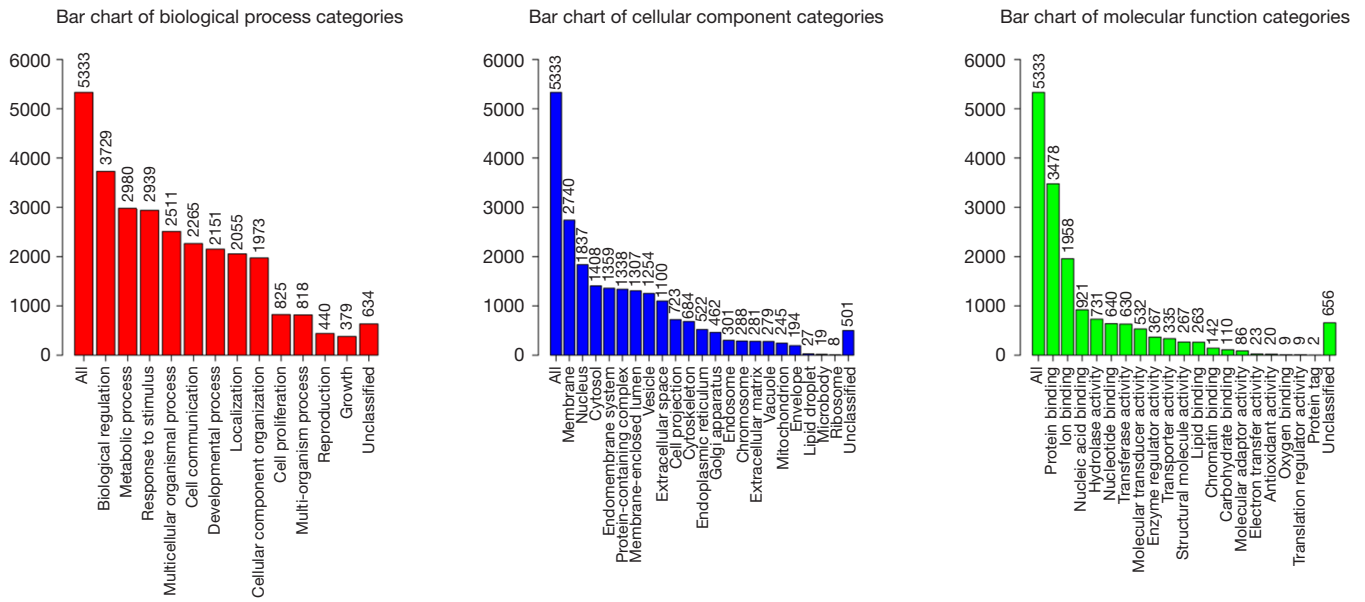
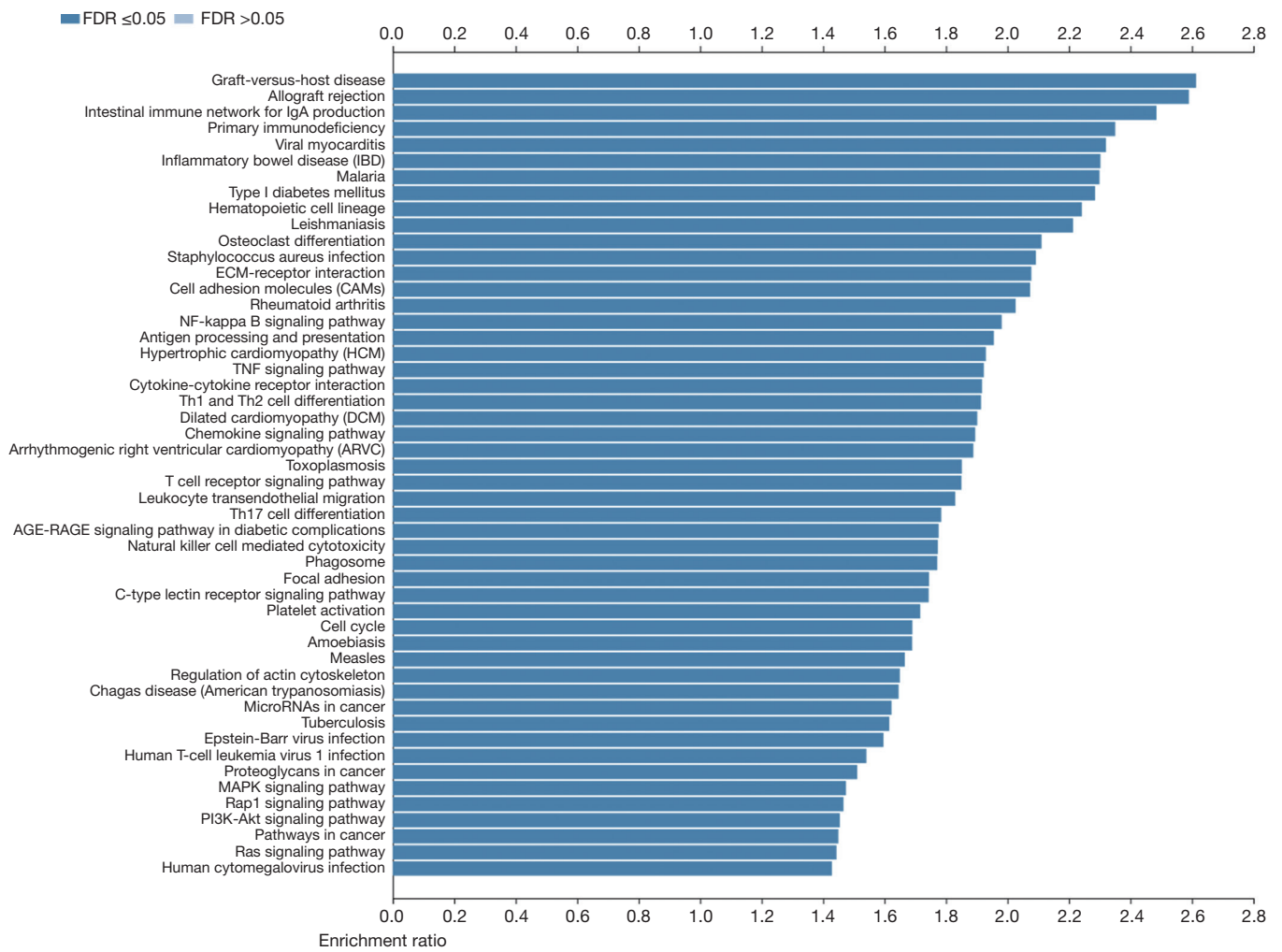**Figure S1** Biological process, cellular component, and molecular function positively correlated with PIM1.

Figure S2 Biological processes.